Pharmaceutical Research, Vol. 26, No. 3, March 2009 (© 2008)
DOI: 10.1007/s11095-008-9775-0

Research Paper

Subambient Behavior of Mannitol in Ethanol–Water Co-solvent System

Akira Takada,[1,4,5] Steven L. Nail,[2] and Masakatsu Yonese[3]

Received May 31, 2008; accepted October 29, 2008; published online November 12, 2008

Purpose. The purpose of this study is to characterize the freezing behavior of mannitol in ethanol–water co-solvent systems in comparison with the corresponding aqueous solution.
Methods. Subambient differential scanning calorimetry (DSC) and microscopy techniques were used to investigate the freezing behavior of mannitol in aqueous solutions and in ethanol–water co-solvent systems.
Results. The DSC thermogram of the frozen aqueous solution, which was warmed after cooling at 5.0°C/min, consisted of a glass transition, an endothermic transition, and a crystallization exotherm from mannitol, respectively. The thermograms of ethanol-containing solutions were different in view of including some thermal events attributable to ethanol hydrates. The glass transition of amorphous mannitol was also observed in the thermograms, but became unclear with increasing ethanol in the co-solvent system. The microscopy experiments enabled understanding of the subambient behavior of mannitol. Ethanol was largely removed by vacuum drying rather than freeze-drying. In addition, such manipulations as annealing during the freezing process and slower cooling (0.5°C/min) enhanced the crystallization of mannitol in the frozen system.
Conclusions. In the presence of ethanol, crystallization of mannitol was inhibited under subambient conditions. Annealing or slower cooling promoted the crystallization of mannitol during the freezing process.

KEY WORDS: co-solvent; DSC; ethanol; mannitol; microscopy.

INTRODUCTION

Mannitol is a widely used excipient in the pharmaceutical industry, and frequently has been selected as a bulking agent, a lyoprotectant, or a cryoprotectant in many freeze-dried formulations. The high eutectic melting point of frozen mannitol aqueous solution (about −1.5°C) allows a high product temperature during primary drying and leads to a faster drying rate and more efficient freeze-drying cycle for commercial products. In addition, freeze-dried products containing mannitol generally are pharmaceutically elegant in their appearance.

Freezing and freeze-drying behavior of drug substances or excipients have been investigated by many scientists (1–4). Such investigations provide a useful rationale for the formulations and the freeze-drying cycles. In development of protein formulations, lyoprotectants, cryoprotectants, and other additives are utilized in order to maintain the integrity of the proteins. Mannitol in aqueous frozen systems has been studied by several investigators. Kett *et al.* examined the subambient behavior of mannitol with low-temperature X-ray diffractometry (XRD), DSC and microscopy (5). They showed that amorphous freeze concentrate co-existed with crystalline mannitol during cooling and that the formation of the mannitol beta polymorph was promoted by annealing. Cavatur *et al.* studied the effect of cooling rate and other excipients on the crystallization behavior of mannitol in aqueous frozen system (6). They concluded that rapid cooling and the presence of additives inhibited the crystallization of mannitol during freezing and that mannitol could be used as a lyoprotectant.

Water and organic solvent mixtures, as co-solvent systems, are sometimes used in parenteral formulations (7). As Teagarden *et al*. discussed in their review (7), the potential advantages of co-solvents in parenteral formulations are increased solubility of poorly water-soluble compounds, enhancement in the stability of the compounds in the formulations, reduction of freeze-drying time, and improvement of reconstitution characteristics. The disadvantages of co-solvents include a limited number of organic solvents with properties, such as freezing point and vapor pressure, that make them acceptable for freeze-drying, potential toxicity concerns due to residual solvent in freeze-dried powder, operator safety, and storage issues, precipitation upon dilution with aqueous fluids, and higher production cost. Tertiary butyl alcohol (TBA) is one of the most popular solvents used in freeze-dried

[1] Pharmaceutical Development Laboratories, Ono Pharmaceutical Co., Ltd., Shimamoto, Osaka, Japan.
[2] Baxter Biopharma Solutions, LLC, Bloomington, Indiana, USA.
[3] Faculty of Pharmaceutical Sciences, Nagoya City University, Nagoya, Aichi, Japan.
[4] 3-1-1, Sakurai, Shimamoto, Mishima, Osaka, 618-8585, Japan.
[5] To whom correspondence should be addressed. (e-mail: a.takada@ono.co.jp)

formulations. Freezing and freeze-drying behavior of ingredients in solutions containing TBA has been evaluated (8–11). Ni *et al.* have demonstrated that TBA improved the stability of an antitumor drug by creating needle-shaped crystals during the freeze-drying process (8). Telang *et al.* studied the effect of TBA on the crystallization and stability of cephalothin sodium (9). The use of TBA resulted in crystalline drug, which increased both stability and pharmaceutical elegance. Isopropyl alcohol (IPA) has also been studied as a co-solvent for pharmaceutical lyophilization. Koyama *et al.* have shown that the crystallization of cafezolin sodium was promoted in the presence of IPA and that solid-state stability was enhanced (12). Ethanol is a typical organic solvent which is easily mixed with water, but there has been little investigation of the application of ethanol/water systems in freeze-dried formulations. It has been reported that the freeze-drying rate of ethanol/water co-solvent systems was slower than the corresponding aqueous system due to incompletely frozen systems when using a conventional pharmaceutical freeze dryer (13). Ethanol is classified in Class 3 of ICH guidelines (14) and the residual ethanol in freeze-dried powder would represent a reasonably low safety risk. Therefore, examination of the use of ethanol/water co-solvent systems in pharmaceutical freeze-drying would seem to be worthwhile. The purpose of this study was to examine the effect of ethanol concentration, cooling rate, and annealing time on freezing and freeze-drying behavior of mannitol in ethanol–water co-solvent systems. Mannitol in aqueous solution was also characterized as a function of cooling rate and annealing time, and the co-solvent systems themselves were investigated to help understand the behavior of mannitol in ethanol–water solutions.

MATERIALS AND METHODS

Materials

D-mannitol (Japanese Pharmacopeias grade) was provided by Kyowa Hakko Kogyo Co., Ltd. (JAPAN) and was used as received. Ethanol used in this study was USP grade (AAPER Alcohol and Chemical Co., Shelbyville, KY). Water was purified by ion exchange, followed by distillation.

Methods

Mannitol solutions were prepared by dissolving the desired weight of mannitol in water, adding a predetermined volume of ethanol, and then adjusting the total volume with water. Therefore, mannitol concentrations in this study were expressed in *w*/*v* %, while ethanol concentrations are expressed as *v*/*v* %. All of the solutions used in this study were filtered with PVDF filter units (Millex (R) -GV, 0.22 μm, Durapore, Millipore Corporation, Bedford, MA) prior to use. DSC measurements for frozen solutions were carried out with a Perkin-Elmer (Norwalk, CT) Pyris 1 instrument equipped with a liquid nitrogen cooling system. The instrument was calibrated using the melting points of indium (156.6°C) and mercury (−38.8°C) and the enthalpy of indium (28.71 J/g). Helium was used as a purge gas at a rate of 20 mL/min. Approximately 10 μL of mannitol solutions were placed in aluminum sample pans. The pans were sealed hermetically for the DSC measurements. The solution samples were cooled to less than −50°C at a rate of 0.5 or 5.0°C/min. Thermograms were recorded during heating at 5.0°C/min.

The solution sample for microscopy was placed on the stage of a polarized light microscope (Olympus BH-2). Approximately 5 μL of solution was placed between two cover slips and the cover slips were placed on the stage. Liquid nitrogen was supplied to the stage with a pump (Model LNP, Linkam Scientific Instruments, Tadworth, Surrey, UK) to cool the samples and the stage temperature was controlled with a separate controller (Model TMS 94, Linkam Scientific Instruments, Tadworth, Surrey, UK). Observations during the freezing and freeze-drying were recorded with a video camera.

RESULTS AND DISCUSSION

Characterization of Mannitol in Aqueous Solution

In the first step of the study, mannitol in aqueous solution was examined as a function of cooling rate, annealing time, and mannitol concentration to compare with the freezing characteristics of mannitol in ethanol-containing solutions. The behavior of mannitol in aqueous solution was investigated with DSC. Five percent (*w*/*v* %) mannitol solutions were first cooled at 5.0°C/min from ambient temperature to −50°C. The solutions were then warmed to ambient temperature at 5.0°C/min. The DSC thermogram during warming consists of a glass transition followed by an endotherm and an exotherm (thermogram A in Fig. 1). The exotherm at −22°C arises from the crystallization of mannitol. It is well known that mannitol readily crystallizes in aqueous solution as reported in previous publications (4,5,15). The glass transition was observed with onset at −32°C in this study. This result is consistent with the above reports. The endotherm at −24°C has been interpreted in various ways. Kett *et al.* concluded, based on modulated DSC experiments, that this thermal event could be an endothermic relaxation accompanied by a glass transition (5). Cavatur *et al.* also examined with oscillatory DSC and concluded that it is a second glass transition but not enthalpic recovery (15).

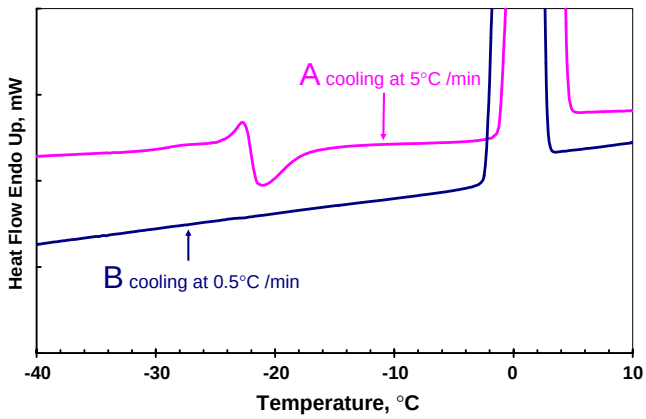

Fig. 1. DSC thermograms of 5% (*w*/*v*) mannitol aqueous solution heated at 5.0°C/min. The solutions were initially cooled from room temperature to −80°C at 5.0°C/min (*A*) and to −50°C at 0.5°C/min (*B*). No thermal event was observed below −40°C. The DSC thermograms are shown only above −40°C.

A DSC thermogram was also obtained at a slower cooling rate of 0.5°C/min. The thermogram during warming had no thermal events from −50°C to ambient temperature except for the endotherm resulting from ice melting (thermogram B in Fig. 1). This result suggests that the crystallization of mannitol is completed during the initial cooling process. The thermogram recorded during cooling at 0.5°C/min in the identical DSC measurement indicated two exotherms. One was a large exotherm attributable to ice crystal formation from supercooled water. The other was a smaller exotherm observed at −14°C, which probably arises from the crystallization of mannitol. Table I shows the enthalpies of crystallization of mannitol during cooling and the subsequent heating process compared with the enthalpies calculated from the DSC thermogram at a cooling rate of 5.0°C/min. The enthalpy values of mannitol crystallization during cooling and heating processes were different, depending on the cooling rate. Therefore, slower cooling tended to promote the crystallization of mannitol in the freezing process. No exotherm attributed to mannitol crystallization was observed during the warming step in the DSC charts at a cooling rate of 0.5°C/min. The same results were obtained at 1% and 10% mannitol concentrations.

Annealing is one of the manipulations used to promote crystallization of amorphous materials in frozen systems. Five percent mannitol solution cooled to −50°C at 5.0°C/min was annealed at −10°C for 10 min in this study. Fig. 2 shows the DSC thermograms during warming before and after annealing. No thermal events appeared in the temperature ranges from −35°C to −10°C after annealing, while complex events were observed in the same region before the annealing. Further investigation would be required to determine the annealing conditions needed in actual freeze-drying, given the effects of scale and uncertainties in heat transfer rates.

To further understand the freezing and freeze-drying behavior of mannitol in aqueous solution, freeze dry microscopy was used. Five percent mannitol aqueous solution was cooled to −70°C at 5°C/min in the first experiment. Ice crystals, which looked dendritic, appeared at approximately −20°C from the supercooled solution in the freezing step (Fig. 3a) and no other change was observed during the subsequent cooling process down to −70°C. In the heating process at 1°C/min with vacuum, a sublimation front was first observed clearly at −35°C and advanced faster as the temperature increased. Many dark dots appeared in the frozen region and grew as the temperature increased (in the dotted circle in Fig. 3d). This observation may be the result of crystallization of mannitol. Such crystals are unclear in Fig. 3c due to the resolution of the photograph, but they could be observed from −15°C with the video camera system used in this study. In addition, the dried area also appeared to change gradually in a temperature range between −25 and −10°C. Fig. 3b and d show pictures of the dried area at −25 and −5°C, respectively. Most of the dried area looked uniformly green at the lower temperature, which was probably caused by birefringence from fine crystals of mannitol. As the temperature increased, the texture changed, and crystals of mannitol appeared more clearly in the dried area. This phenomenon probably resulted from crystal growth of mannitol due to the annealing effect. This is also consistent with the thermal events observed between −25 and −10°C in the DSC measurement (thermogram A in Fig. 1), indicating that mannitol crystallized in such a temperature range. No collapse in the dried area was found up to a eutectic melt of the water and mannitol mixture at −1.6°C.

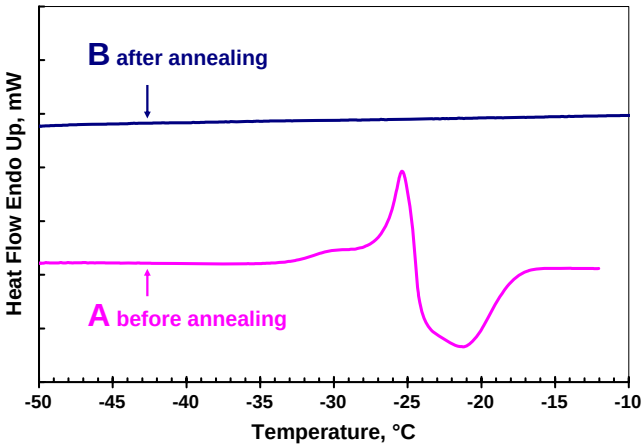

Fig. 2. DSC thermograms of 5% (*w/v*) mannitol aqueous solution before (*A*) and after (*B*) annealing. The solution was cooled to −50°C at 5.0°C/min and then annealed at −10°C for 10 min.

Characterization of Mannitol in Ethanol–Water Co-solvent Systems

The behavior of mannitol in ethanol containing solutions was examined with DSC and microscopy, and compared with

Table I. Crystallization of Mannitol as a Function of Mannitol Concentration and Cooling Rate

Mannitol concentration (*w/v* %)	Cooling at 5.0°C/min				Cooling at 5.0°C/min			
	Cooling		Heating		Cooling		Heating	
	Peak temp. (°C)	ΔH (J/ g)	Peak temp. (°C)	ΔH (J/ g)	Peak temp. (°C)	ΔH (J/ g)	Peak temp. (°C)	ΔH (J/ g)
1	[a]	[a]	n.d	n.d	−36.0	0.601	[a]	[a]
5	−13.9	11.472	n.d	n.d	−34.0	2.547	−21.8	9.178
10	−17.2	28.159	n.d	n.d	−36.2	5.808	−21.6	19.861

[a] The peaks were observed on the thermograms, but they were too small to be calculated
n.d Not detected

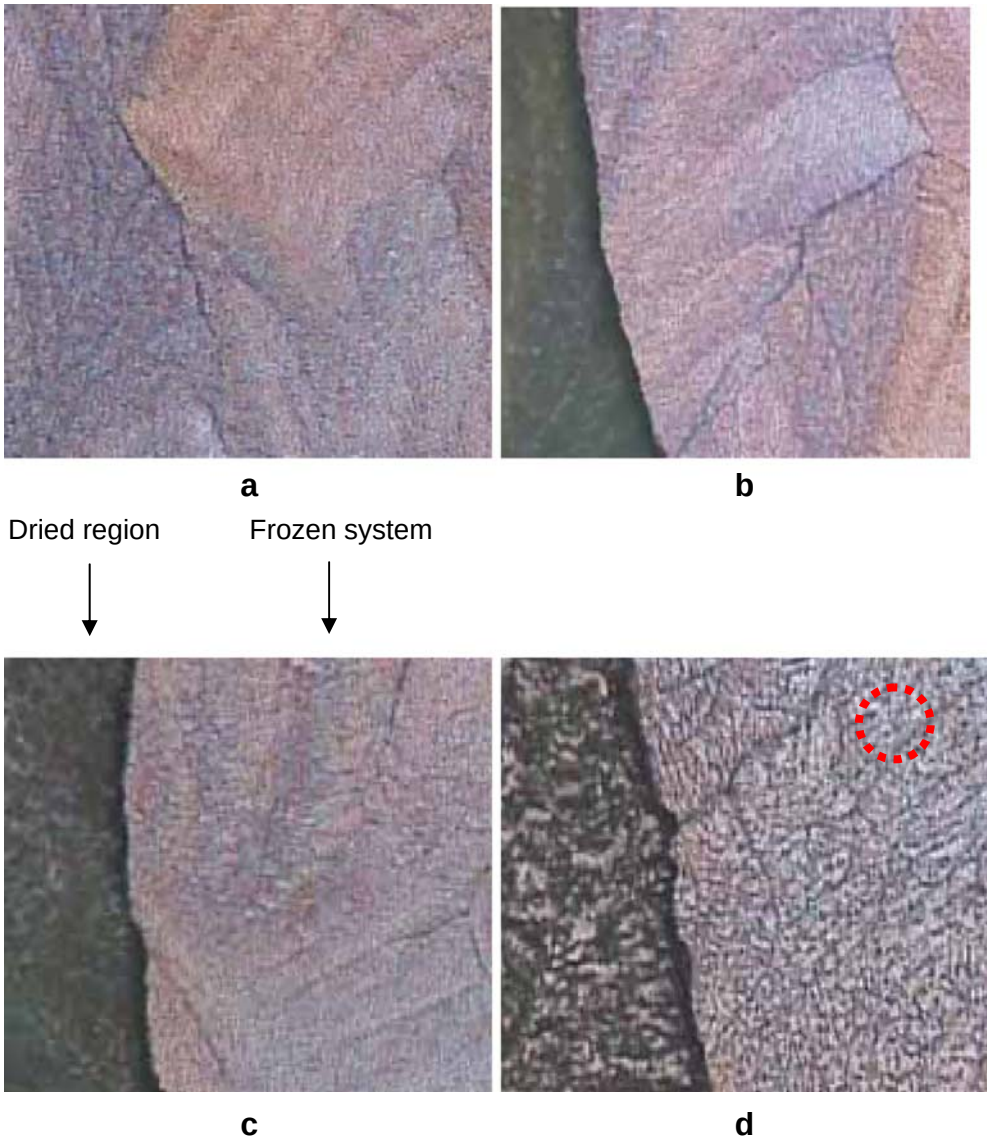

Fig. 3. Microscopy images of 5% (*w*/*v*) mannitol aqueous solution at −50°C in the initial cooling step at 5.0°C/min (**a**); at −25°C (**b**); at −15°C (**c**); at −5°C (**d**) during the subsequent heating. Many dark spots appeared and grew as the temperature increased as seen in the *dotted circle*.

mannitol in aqueous solution. The first cycle in the DSC experiment consisted of ramping at 5.0°C/min from room temperature to −150°C and subsequent heating back to ambient. The DSC thermograms during heating are shown in Fig. 4. There was no thermal event below −80°C in any thermograms, and Fig. 4 illustrates the traces in the range above −80°C. The thermograms are similar to the thermogram of the aqueous solution (thermogram A in Fig. 1) in the sense that a glass transition and a subsequent endotherm are observed. The glass transition and the subsequent endotherm are interpreted as the same behaviors as discussed above for the aqueous solution: Both the glass transition and the endotherm shifted to lower temperature and became broader as the ethanol ratio in the co-solvent increased. On the other hand, there was a significant difference for the DSC profile of 40% ethanol solution from the solutions containing 30% or less ethanol. The DSC thermograms for 30% or less ethanol solution contained an endotherm at around −75°C, while

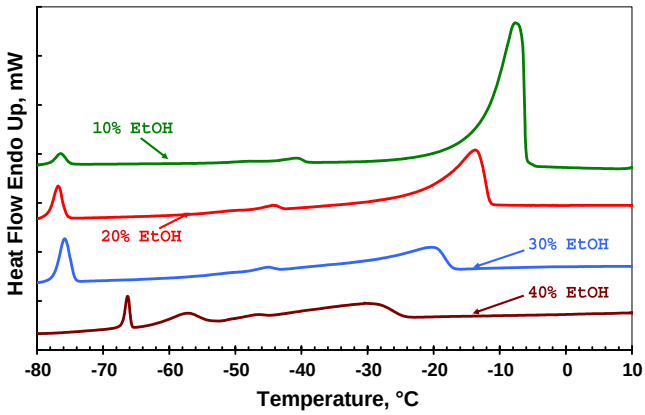

Fig. 4. DSC thermograms of 5% (*w*/*v*) mannitol containing various amounts of ethanol ranged from 10 to 40% (*v*/*v*) heated at 5.0°C/min. The solutions were initially cooled from room temperature to −80°C at 5.0°C/min.

there were two endotherms at −66°C and −57°C in the 40% ethanol solution.

Some experiments were carried out to investigate subambient behavior of ethanol and water co-solvent systems not containing mannitol by DSC. The understanding of the solvent behavior under subambient conditions is important in order to understand the freezing and freeze-drying behavior of mannitol in the ethanol–water co-solvent system. The co-solvents used in this study were prepared in the range of 0 to 50% ethanol. All the solutions were cooled to −140°C at 5.0°C/min and warmed to ambient temperature at 5.0°C/min. Fig. 5 illustrates DSC curves during warming. There were no thermal events below −120°C, and the thermograms above −120°C are shown in Fig. 5. In all the thermograms for the samples containing ethanol, a broad endotherm was observed at a temperature between −50°C and 5°C. The endotherms are attributed to melting of ice, as shown in an ethanol–water phase diagram (Fig. 6) which has been described by Takaizumi (16). They became broader and shifted to lower temperature with increasing ethanol. The shift of the endotherms to lower temperatures corresponds to the melting point depression of ice due to the addition of ethanol.

Other thermal events, which were found at lower temperatures illustrated in Fig. 5, show different patterns as the ethanol concentration increases. The phase diagram in Fig. 6 helps in understanding the DSC thermograms of ethanol/water systems. The thermograms of the 20% and 30% ethanol solutions in Fig. 5 reveal an endotherm at −72°C, which probably arises from the decomposition of peritectic ethanol 5.67-hydrate, as reported by Takaizumi *et al.* (17) and Ott *et al.* (18). In the DSC thermograms of 40% and 50% ethanol, two endotherms at −63°C and −60°C following an exotherm at −90°C are present, while no endotherm was observed at −72°C. The endotherms at −63°C and −60°C appear to correspond to the melting of ethanol monohydrate and the melting of metastable solid other than hexagonal ice that was first formed on cooling, respectively. In addition, the exotherm at −90°C is probably caused by the crystallization of the ethanol monohydrate. A study by Takamuku *et al.* (19) also supports the thermal analysis data

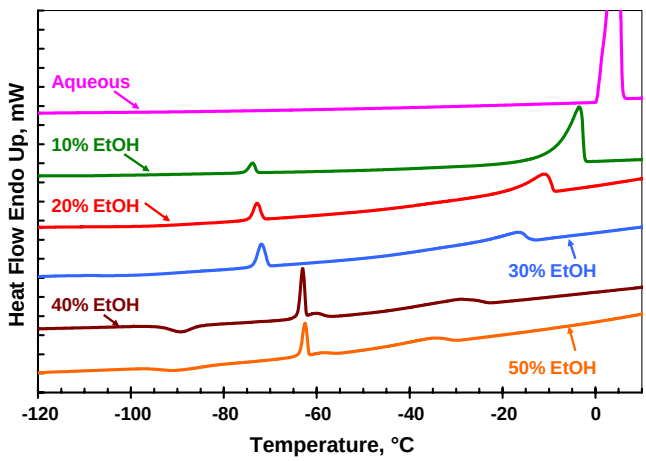

Fig. 5. DSC thermograms of 0 to 50% (*v*/*v*) ethanol heated at 5.0°C/min. The solutions were initially cooled from room temperature to−150°C at 5.0°C/min.

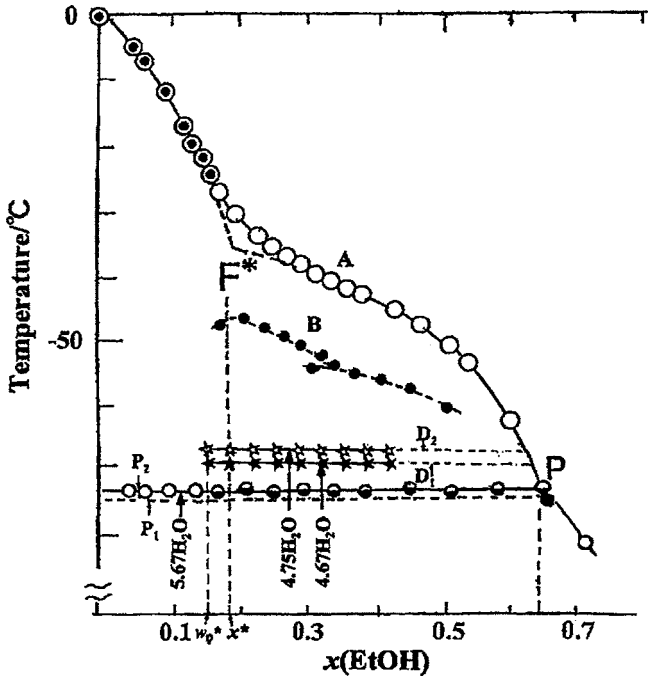

Fig. 6. Liquid–solid phase diagram of ethanol–water composite system. *A* Ice, *B* initially formed solid from super-cooled liquid, P_1 clathrate I, P_2 clathrate II, D_1 new ethanol hydrate I, D_2 new ethanol hydrate II, F^* inflection point, x^* mole fraction for inflection point, *P* peritectic point, w_D^* refers to the concentration from where the hydrates D_1 and D_2 begin to exist. This phase diagram was described by Takaizumi (16).

in this study in the sense that there are significant differences in the solvent behavior between 30% and 40% ethanol. They have reported in their study with X-ray diffractometry that an ethanol–water mixture at 0.1 in mole fraction of ethanol, where tetrahedral-like structure of water was predominantly formed at 25°C, was frozen into hexagonal ice, while ethanol–water mixtures at 0.2 and 0.3 in mole fraction of ethanol, where ethanol chain clusters were mainly formed at 25°C, crystallized as ethanol hydrate. Mole fractions of 0.1 and 0.2 in their study correspond to approximately 26% and 44% (*v*/*v*) ethanol in this study, respectively. The thermal data obtained in this study are also consistent with the data reported by Boutron *et al.* (20). Boutron *et al.* concluded that the exotherm at −90°C corresponded to an ordering of ethanol molecules from a solution containing clathrate cages, and that two endotherms at −63°C and −60°C correspond to a fusion of the hydrate and crystallization of a clathrate from a solution containing only ice crystals, respectively. Thus, ethanol and water molecules interact in the co-solvent systems and the behavior becomes different as the relative concentration of ethanol changes.

Thermal analysis of ethanol–water systems is useful in understanding the system mannitol/ethanol/water. The endotherm at −75°C in the thermograms (Fig. 4) for less than 30% ethanol is attributed to the decomposition of peritectic ethanol hydrate. The enthalpies calculated from the areas of the endotherms increase as the ethanol ratio increases. Two endotherms at −66°C and −57°C in the thermogram of the 40% ethanol solution can be presumed to be the behaviors of the co-solvent system, which are the melting of ethanol

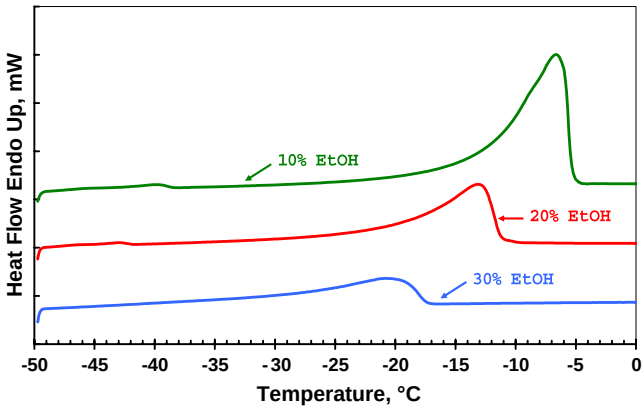

Fig. 7. DSC thermograms of 5% (*w*/*v*) mannitol containing various amounts of ethanol ranged from 10 to 30% (*v*/*v*) heated at 5.0°C/min. The solutions were initially cooled from room temperature to −50°C at 0.5°C/min.

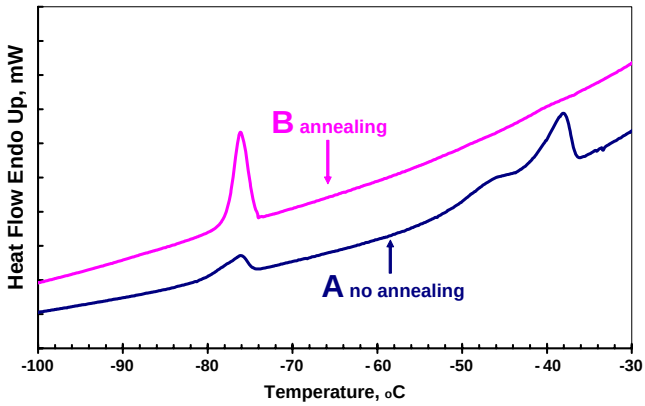

Fig. 8. DSC thermograms of 10% (*w*/*v*) mannitol containing 10% (*v*/*v*) ethanol heated at 5.0°C/min before (*A*) and after (*B*) annealing at −30°C for 10 min.

hydrate and the melting of metastable solid other than hexagonal ice that was first formed on cooling, respectively, as discussed above. Thus, the individual thermal events in the complex DSC thermograms of the mannitol/ethanol/water three constituent solutions illustrated in Fig. 4 are consistent with the behaviors of mannitol and ethanol in water.

Additional DSC experiments were performed to obtain a better understanding of mannitol behavior in the co-solvent system. The variables examined were cooling rate, annealing time, and mannitol concentration. The solutions were cooled to −50°C at a slower cooling rate, 0.5°C/min. Fig. 7 shows thermograms of mannitol solutions containing varying amounts of ethanol, which were obtained during heating at 5.0°C/min. A slight glass transition and endotherm is present at around −40°C in both 10 and 20% ethanol solution. However, the heat capacities and enthalpies calculated for both events were smaller than those obtained at faster cooling rates, 5.0°C/min (as shown in Table II). In contrast, no thermal event was observed in the same temperature range for 30% ethanol. These results suggested that slower cooling promotes the crystallization of mannitol in the ethanol/water co-solvent, as seen in the aqueous solution, but is not completed during cooling for 10 and 20% ethanol solutions. In addition, enthalpies of the endotherms tended to decrease as ethanol concentration increased, indicating that mannitol tends to crystallize during the cooling step as the ethanol ratio in co-solvent system increases.

The next DSC experiments were conducted to understand the effect of annealing time on the freezing behavior of mannitol in ethanol-water co-solvents. The following cycle was used in these measurements: the solution was cooled at 5.0°C/min, annealed at −30°C for 10 min and then reheated at 5.0°C/min. Fig. 8 shows representative thermograms during heating both before and after annealing for 10% mannitol in 10% ethanol solution. The glass transition and the endotherm present with no annealing in the temperature ranges between −60°C and −35°C disappeared after annealing. This is a result of the effect of annealing on crystallization of mannitol in the co-solvent systems, which was an identical phenomenon as shown in the aqueous solution. In addition, annealing increased the intensity of the endotherm at −76°C, which is attributable to melting of ethanol hydrate. The formation of ethanol hydrate is promoted as the crystallization of mannitol increases. Mannitol crystallization results in exclusion of ethanol and water molecules from the crystal lattice of mannitol, and this frees ethanol and water and promotes hydrate formation. Conversely, ethanol molecules may inhibit crystallization of mannitol. Yoshinari *et al.* stated that the hydrogen bonds between mannitol molecules were significant for the crystallization of mannitol, and that boric acid interacts with mannitol molecules and inhibits the formation of hydrogen bonds between mannitol molecules and consequent mannitol crystallization (21). Such a mechanism for inhibition of mannitol crystallization can probably be applied

Table II. Crystallization of Mannitol as a Function of Ethanol Concentration and Cooling Rate

Ethanol concentration (*v*/*v* %)	Heat capacities at Tg' (J/g/°C) Cooling rate (°C/min)		Enthalpies of endotherm (J/g) Cooling rate (°C/min)	
	0.5	5.0	0.5	5.0
0	n.d.	0.405	n.d.	2.223
10	n.d.	0.624	2.111	2.780
20	0.235	0.801	0.745	2.666
30	n.d.	0.749	n.d.	2.041
40	–	n.d.	–	n.d.

n.d: not detected

Fig. 9. Microscopy images of 5% (*w*/*v*) mannitol in 10% (*v*/*v*) ethanol-containing solution at −23°C in the initial cooling step at 5.0°C/min (**a**); at −30°C during the annealing (**b**).

to the ethanol-containing system. In other words, ethanol molecules may interact with mannitol molecules and thus inhibit mannitol crystallization.

Crystallization of mannitol in the ethanol–water co-solvents was also observed microscopically. The temperature program of the microscopy experiment consisted of cooling to −80°C at 5°C/min, annealing for 10 minutes at −30°C, and reheating at 1°C/min through ice melting. Photomicrographs of 5% mannitol solution in 10% ethanol are presented in Fig. 9. In the first cooling step, ice crystals appeared at −23°C (Fig. 9a), but no other change was seen during this process. Mannitol crystallized during annealing at −30°C as shown by development of the darker regions illustrated in Fig. 9b. These crystalline regions grew gradually during annealing. The temperature range at which the mannitol crystallization occurred is close to the region where a glass transition and an endotherm appear in the DSC thermograms (Fig. 4). No clear exotherm was observed in the DSC thermogram, but mannitol seemed to crystallize at a temperature just above the glass transition of the amorphous mannitol, as observed in the aqueous solution. The mannitol solutions in 20, 30 and 40% ethanol co-solvents were also subjected to microscopic experiments under the same conditions. The observations were very similar to that for the 10% ethanol solution. In addition, the temperatures at which the crystallizations were demonstrated in the microscopic observation were consistent with the thermal events seen in the DSC experiments.

The next microscopy experiments were performed with vacuum to observe the freeze-drying behavior of mannitol. Five percent mannitol solution in 10% ethanol was cooled to −80°C and then warmed to ambient temperature under vacuum. Bubbles appeared in the frozen system at −80°C and expanded with increasing temperature, as shown in Fig. 10 (at −30°C). This observation is consistent with melting of the ethanol hydrate. The microscopy experiments with vacuum also revealed collapse of the dried mannitol around the sublimation interface. Such a collapse of amorphous mannitol in 10% ethanol was observed at −31°C as shown in Fig. 10. On the other hand, the glass transition temperature of mannitol in 10% ethanol solution was estimated to be −52°C from the DSC measurement. The collapse temperature and the glass transition temperature of mannitol at various ethanol ratios are summarized in Table III. The increase in ethanol ratio in the solvent tended to decrease both the collapse

Fig. 10. Microscopy images of 5% (*w*/*v*) mannitol in 10% (*v*/*v*) ethanol-containing solution at −30°C.

Table III. Collapse and Glass Transition Temperatures of Mannitol in Ethanol–Water Co-Solvent System

Ethanol Concentration (*v*/*v* %)	Collapse Temperature (°C) from Microscopy	Glass Transition Temperature (°C) from DSC
0	Not observed	−32
10	−33	−52
20	−32	−55
30	−37	−57
40	−37	[a]

[a] Not detected clearly due to overlap with another endotherm peak

temperature and the glass transition temperature. This may be explained by a role of ethanol as a plasticizer. For the solutions containing ethanol, the differences between the collapse temperature and the glass transition temperature were larger than the difference observed in aqueous systems. This arose from the fact that the collapse was observed by microscopy in the dried material, which contains lower level of ethanol than the frozen system. In contrast, the glass transitions in DSC measurements were observed in the frozen system containing more ethanol than in dried region which the collapse was found. Therefore, these results demonstrated that ethanol was removed with vacuum during the initial stage of the drying process.

Finally, the implementation of lyophilization with general freeze-dryers for ethanol-containing mannitol formulations is discussed. In general, commercial freeze-dryers are capable of cooling; only to around −50°C at which ethanol is in the unfrozen state. Although all components including ethanol should be ideally in frozen state prior to vacuum drying process, it is not achievable to freeze ethanol sufficiently with commonly-used freeze-dryers due to lower freezing point of ethanol. Insufficient frozen solution in lyophilization process can cause abrupt boiling of ethanol under vacuum, resulting in powder blow-out from vials during freeze-drying. In addition, product temperature should be reduced below collapse temperature during the drying process to obtain pharmaceutically acceptable freeze-dried cake. In these points of view, the amount of ethanol to be added in ethanol-containing mannitol formulations should be theoretically minimized to have successful freeze-drying. In author's experiences, up to 30% ethanol allowed elegant freeze-dried cakes with a laboratory scale freeze dryer. However, elegance of freeze-dried cakes and success of lyophilization can depend on lots of factors: ethanol ratio, freeze-drying variables, magnitude of freeze dryer, mannitol concentration, characteristics of active pharmaceutical ingredients, *etc*. Detailed investigation is necessary to optimize formulation and freeze drying cycle considering each formulation.

CONCLUSION

The study presented here clearly demonstrates that ethanol inhibited mannitol crystallization during freeze-drying. This tendency increased with increasing ethanol in the solutions. Thus, ethanol would be expected to enhance the role of mannitol as a cryoprotectant or a lyoprotectant in freeze dried formulations when it is used to increase the solubility of poorly water-soluble drug substances, enhance the stability of the compounds in the formulations, reduce freeze-drying time, and improve reconstitution characterization. Manipulations like annealing or slower cooling are necessary to promote crystallization of mannitol in solutions containing ethanol.

ACKNOWLEDGEMENTS

The authors gratefully acknowledge Ono pharmaceutical Co., Ltd. for financial support. We also thank Purdue University for the opportunity to carry out this research.

REFERENCES

1. A. Martini, S. Kume, M. Crivellente, and R. Artico. Use of subambient differential scanning calorimetry to monitor the frozen-state behavior of blends of excipients for freeze-drying. *PDA J. Parenter. Sci. Technol*. **51**:62–67 (1997).
2. K. Kasraian, T. M. Spitznagel, J. A. Juneau, and K. Yim. Characterization of the sucrose/glycine/water system by differential scanning calorimetry and freeze-drying microscopy. *Pharm. Dev. Technol*. **3**:233–239 (1998). doi:10.3109/10837459809028500.
3. S. Chongprasert, S. A. Knopp, and S. L. Nail. Characterization of frozen solutions of glycine. *J. Pharm. Sci*. **90**:1720–1728 (2001). doi:10.1002/jps.1121.
4. K. Izutsu, S. O. Ocheda, N. Aoyagi, and S. Kojima. Effects of sodium tetraborate and boric acid on nonisothermal mannitol crystallization in frozen solutions and freeze-dried solids. *Int. J. Pharm*. **273**:85–93 (2004). doi:10.1016/j.ijpharm.2003. 12.024.
5. V. L. Kett, S. Fitzpatrick, B. Cooper, and D. Q. M. Craig. An investigation into the subambient behavior of aqueous mannitol solutions using differential scanning calorimetry, cold stage microscopy, and x-ray diffractometry. *J. Pharm. Sci*. **92**:1919–1929 (2003). doi:10.1002/jps.10449.
6. A. Pyne, R. Surana, and R. Suryanarayanan. Crystallization of mannitol below Tg' during freeze-drying in binary and ternary aqueous systems. *Pharm. Res*. **19**:901–908 (2002). doi:10.1023/A:1016129521485.
7. D. L. Teagarden, and D. S. Baker. Practical aspects of lyophilization using non-aqueous co-solvent systems. *Eur. J. Pharm. Sci*. **15**:115–133 (2002). doi:10.1016/S0928-0987(01)00221-4.
8. N. Ni, M. Tesconi, S. E. Tabibi, S. Gupta, and S. H. Yalkowsky. Use of pure t-butanol as a solvent for freeze-drying: a case study. *Int. J. Pharm*. **226**:39–46 (2001). doi:10.1016/S0378-5173(01)00757-8.
9. C. Telang, and R. Suryanarayanan. Crystallization of cephalothin sodium during lyophilization from tert-butyl alcohol–water cosolvent system. *Pharm. Res*. **22**:153–160 (2005). doi:10.1007/s11095-004-9021-3.
10. J. Oesterle, F. Franks, and T. Auffret. The influence of tertiary butyl alcohol and volatile salts on the sublimation of ice from frozen sucrose solutions: implications for freeze-drying. *Pharm. Dev. Technol*. **3**:175–183 (1998). doi:10.3109/10837459809028493.
11. S. Wittaya-Areekul, G. F. Needham, N. Milton, M. L. Roy, and S. L. Nail. Freeze-drying of tert-butanol/water cosolvent systems: a case report on formulation of a friable freeze-dried powder of tobramycin sulfate. *J. Pharm. Sci*. **91**:1147–1155 (2002). doi:10.1002/jps.10113.
12. Y. Koyama, M. Kamat, R. J. De Angelis, R. Srinivasan, and P. P. DeLuca. Effect of solvent addition and thermal treatment on freeze drying of cefazolin sodium. *J. Parenter. Sci. Technol*. **42**:47–52 (1988).
13. H. Seager, C. B. Taskis, M. Syrop, and T. J. Lee. Structure of products prepared by freeze-drying solutions containing organic solvents. *J. Parenter. Sci. Technol*. **39**:161–179 (1985).
14. International Conference on Harmonization guidance Q3C impurities: guideline for residual solvents.
15. R. K. Cavatur, N. M. Vemuri, A. Pyne, Z. Chrzan, D. Toledo-Velasquez, and R. Suryanarayanan. Crystallization behavior of mannitol in frozen aqueous solutions. *Pharm. Res*. **19**:894–900 (2002). doi:10.1023/A:1016177404647.
16. K. Takaizumi. A curious phenomenon in the freezing–thawing process of aqueous ethanol solution. *J. Sol. Chem*. **34**:597–612 (2005). doi:10.1007/s10953-005-5595-6.
17. K. Takaizumi, and T. Wakabayashi. The freezing process in methanol-, ethanol-, and propanol-water systems as revealed by differential scanning calorimetry. *J. Sol. Chem*. **26**:927–939 (1997). doi:10.1007/BF02768051.
18. J. B. Ott, J. R. Goates, and B. A. Waite. (Solid+liquid) phase equilibria and solid-hydrate formation in water+methyl, +ethyl, +isopropyl, and +tertiary butyl alcohols. *J. Chem. Thermodynamics*. **11**:739–746 (1979). doi:10.1016/0021-9614(79)90109-5.

19. T. Takamuku, K. Saisho, S. Nozawa, and T. Yamaguchi. X-ray diffraction studies on methanol–water, ethanol–water, and 2-propanol–water mixtures at low temperatures. *J. Molecular Liquids*. **119**:133–146 (2005). doi:10.1016/j.molliq.2004.10.020.
20. P. Boutron, and A. Kaufmann. Metastable states in the system water–ethanol. Existence of a second hydrate; curious properties of both hydrates. *J. Chem. Phys*. **68**:5032–5041 (1978). doi:10.1063/1.435619.
21. T. Yoshinari, R. T. Forbes, P. York, and Y. Kawashima. Crystallisation of amorphous mannitol is related using boric acid. *Int. J. Pharm*. **258**:109–120 (2003). doi:10.1016/S0378-5173(03)00155-8.